Molecular Biology of the Cell
Vol. 17, 1723–1733, April 2006

Splicing Speckles Are Not Reservoirs of RNA Polymerase II, but Contain an Inactive Form, Phosphorylated on Serine^2 Residues of the C-Terminal Domain[D]

Sheila Q. Xie,* Sonya Martin,*† Pascale V. Guillot,*‡ David L. Bentley,§ and Ana Pombo*

*Medical Research Council Clinical Sciences Centre, Faculty of Medicine, Imperial College London, Hammersmith Hospital Campus, London W12 0NN, United Kingdom; and §Department of Biochemistry and Molecular Genetics, University of Colorado Health Sciences Center, University of Colorado School of Medicine, Aurora, CO 80045

Submitted August 5, 2005; Revised January 26, 2006; Accepted January 30, 2006
Monitoring Editor: A. Gregory Matera

"Splicing speckles" are major nuclear domains rich in components of the splicing machinery and polyA$^+$ RNA. Although speckles contain little detectable transcriptional activity, they are found preferentially associated with specific mRNA-coding genes and gene-rich R bands, and they accumulate some unspliced pre-mRNAs. RNA polymerase II transcribes mRNAs and is required for splicing, with some reports suggesting that the inactive complexes are stored in splicing speckles. Using ultrathin cryosections to improve optical resolution and preserve nuclear structure, we find that all forms of polymerase II are present, but not enriched, within speckles. Inhibition of polymerase activity shows that speckles do not act as major storage sites for inactive polymerase II complexes but that they contain a stable pool of polymerase II phosphorylated on serine^2 residues of the C-terminal domain, which is transcriptionally inactive and may have roles in spliceosome assembly or posttranscriptional splicing of pre-mRNAs. Paraspeckle domains lie adjacent to speckles, but little is known about their protein content or putative roles in the expression of the speckle-associated genes. We find that paraspeckles are transcriptionally inactive but contain polymerase II, which remains stably associated upon transcriptional inhibition, when paraspeckles reorganize around nucleoli in the form of caps.

INTRODUCTION

The cell nucleus is a complex organelle that harbors chromosomes organized into territories as well as many subcompartments rich in protein complexes with roles in DNA and RNA metabolism. "Splicing speckles," or interchromatin granule clusters at the ultrastructural level, are major nuclear domains that are rich in components of the splicing machinery and polyA$^+$ RNA (Lamond and Spector, 2003), but they also contain other nuclear proteins with roles in RNA metabolism and transcription, including RNA polymerase II (pol II) and CDK9 (Mintz *et al*., 1999; Herrmann and Mancini, 2001). Speckles are often found spatially associated with "paraspeckle" domains, which are marked by paraspeckle proteins (PSPs) 1 and 2 (Fox *et al*., 2002). The protein content of paraspeckles suggests that they are involved in RNA synthesis or processing; PSPs interact with the splicing and transcription factor-associated proteins p54nrb/NonO and PSF, respectively, which in turn interact with pol II (Emili *et al*., 2002; Kameoka *et al*., 2004; Myojin *et al*., 2004; Fox *et al*., 2005).

The discovery that the association of splicing factors and polyA$^+$ RNA with speckles is highly dynamic has suggested that these domains are metastable compartments (Kruhlak *et al*., 2000; Phair and Misteli, 2000; Molenaar *et al*., 2004). However, speckles remain stable in unfixed permeabilized cells for many hours and resist biochemical purification (Mintz *et al*., 1999), such that some of their components are likely to be structural. Although speckles are mostly devoid of chromatin and are not major sites of transcription, as measured after incorporation of labeled nucleotides into nascent RNAs (Puvion and Puvion-Dutilleul, 1996; Iborra *et al*., 1998; Cmarko *et al*., 1999), specific mRNA-coding genes and gene-rich R bands have been found preferentially associated with them (Clemson and Lawrence, 1996; Johnson *et al*., 2000; Shopland *et al*., 2002, 2003; Moen *et al*., 2004). That unspliced mRNAs are present and further accumulate upon splicing inhibition (Johnson *et al*., 2000) suggests a role for speckles in gene expression and possibly posttranscriptional

This article was published online ahead of print in *MBC in Press* (http://www.molbiolcell.org/cgi/doi/10.1091/mbc.E05–08–0726) on February 8, 2006.

[D] The online version of this article contains supplemental material at *MBC Online* (http://www.molbiolcell.org).

Present addresses: † Tenovus Research Laboratory, University of Southampton, Southampton General Hospital, Southampton SO15 5PA, United Kingdom; ‡ Institute of Reproductive and Developmental Biology, Imperial College London, London W12 0NN, United Kingdom.

Address correspondence to: Ana Pombo (ana.pombo@csc.mrc.ac.uk).

Abbreviations used: AP, alkaline phosphatase; Br-RNA, bromo-UTP–labeled RNA; CTD, C-terminal domain; DRB, 5,6-dichloro-1-β-D-ribofuranosylbenzimidazole; EGFP, enhanced green fluorescent protein; IF, immunofluorescence; pol II, RNA polymerase II; pol II_A, hypophosphorylated polymerase II; pol II_O, hyperphosphorylated polymerase II; PSP, paraspeckle protein; Ser^2P, phosphorylated serine^2 residues of the CTD; Ser^5P, phosphorylated serine^5 residues of the CTD; SR, serine/arginine; WB, Western blot.

Supplemental Material can be found at:
http://www.molbiolcell.org/content/suppl/2006/02/07/E05-08-0726.DC1.html

splicing of pre-mRNAs for which splicing is not completed cotranscriptionally.

Messenger RNAs and some small structural RNAs are transcribed by pol II. Its largest subunit (RPB1) contains an unusual C-terminal domain (CTD) with multiple tandem heptad repeats of consensus sequence $Tyr^1Ser^2Pro^3Thr^4Ser^5Pro^6Ser^7$ (52 repeats in mammals), which is required for RNA processing (Maniatis and Reed, 2002; Zorio and Bentley, 2004) and for recruitment of splicing factors to sites of transcription (Misteli and Spector, 1999). Phosphorylation of the CTD correlates with steps of the transcription cycle; hypophosphorylated pol II is thought to bind to promoters, becoming phosphorylated on Ser^5 residues during transcription initiation and on Ser^2 once elongation begins (Kobor and Greenblatt, 2002). Several studies have reported enrichment of Ser^2P pol II in splicing speckles relative to the nucleoplasm (Bregman *et al*., 1994, 1995; Bisotto *et al*., 1995; Mortillaro *et al*., 1996; Zeng *et al*., 1997; Patturajan *et al*., 1998; Mintz and Spector, 2000), proposing a model in which speckles serve as reservoirs of polymerase complexes that are mobilized to supply sites of active transcription. In contrast, other reports indicate a homogeneous distribution of Ser^2P pol II throughout the nucleoplasm (Grande *et al*., 1997; Zeng *et al*., 1997). These different results may depend on experimental differences such as the antibodies used and cell preparation conditions (Guillot *et al*., 2004). Although, live cell experiments using enhanced green fluorescent protein (EGFP)-tagged RPB1 reveal a homogeneous distribution of pol II throughout the nucleoplasm (Sugaya *et al*., 2000; Kimura *et al*., 2002), these experiments do not exclude the possibility that some forms of the enzyme might be enriched, or cycle through splicing speckles.

Here, we have examined the role of splicing speckles as reservoirs of pol II by systematic localization of the differently phosphorylated forms of pol II in the nucleus of control and transcriptionally inhibited HeLa cells. We show that splicing speckles are not major sites of pol II storage, although they contain a small population of Ser^2P pol II complexes that are stably bound but transcriptionally inactive. We also characterize the pol II content and transcriptional activity of the speckle-associated paraspeckle domains.

MATERIALS AND METHODS

Cell Culture, Bromo-UTP–labeled RNA (Br-RNA) Labeling, Fixation and Ultrathin (Tokuyasu) Cryosectioning

HeLa cells were grown in 5% CO_2 at 37°C in DMEM, supplemented with 10% heat-inactivated fetal calf serum, 2 mM L-glutamine, 100 IU/ml penicillin, 100 μg/ml streptomycin, and 20 mM HEPES (all from Invitrogen, Paisley, United Kingdom). α-Amanitin (α-am) (50 μg/ml; Sigma Chemical, Poole, Dorset, United Kingdom) was added to cultures for 5 h before fixation or whole cell extract preparation.

To label sites of transcription, cells were permeabilized with saponin in a "physiological buffer" containing bovine serum albumin (BSA), and incubated (15 min) in 0.1 M Br-UTP and the other NTPs before fixation (Pombo *et al*., 1999b). Cells were fixed in 4% freshly depolymerized paraformaldehyde in 250 mM HEPES (pH 7.6; 10 min; 4°C), refixed in 8% paraformaldehyde in 250 mM HEPES (pH 7.6; 2 h; 4°C), scrapped, and pelleted during the latter fixation (Pombo *et al*., 1999a). Pellets were embedded (2 h) in 2.1 M sucrose in phosphate-buffered saline (PBS), transferred onto a copper block, frozen, and stored in liquid nitrogen. Cryosections (100–150 nm in thickness) were cut with a glass knife using an ultracryomicrotome (UltraCut UCT52; Leica, Milton Keynes, United Kingdom), captured on drops of 2.1 M sucrose in PBS, transferred to 0.17-mm-thick coverslips for immunofluorescence, and used immediately or stored at −20°C.

Antibodies

Primary antibodies to the largest subunit of pol II were as follows. H224 was raised against recombinant protein corresponding to amino acids 1-224 at the amino terminus (rabbit IgG; 1:100 [Western blot; WB] and 1:10 [immunofluorescence, IF]; Santa Cruz Biotechnology, Santa Cruz, CA). ARNA-3 recognizes an epitope delineated by amino acids 794-822 outside the CTD (mouse IgG; 1:500 [WB] and 1:50 [IF]; Research Diagnostics, Flanders, NJ]. 8WG16 preferentially recognizes nonphosphorylated heptads of the CTD (mouse IgG; 1:100 [WB and IF]; BioDesign International, Saco, ME; Patturajan *et al*., 1998; Cho *et al*., 2001). Although some 8WG16 batches have been reported to contain significant cross-reactivity to faster migrating bands (Bregman *et al*., 1995), the one used here shows only a relatively minor reaction with an additional band (Figure 1B, arrow). Rabbit anti-Ser^5P recognizes phosphorylated Ser^5 peptides (rabbit IgG; 1:3000 [WB] and 1:1000 [IF]; Schroeder *et al*., 2000]. 4H8 was raised against phosphorylated Ser^5 (mouse IgG; $1:2 \times 10^5$ [WB] and 1:500 [IF]; Upstate Biotechnology, Lake Placid, NY]. H5 recognizes phosphorylated Ser^2 (mouse IgM; 1:500 [WB] and 1:2000 [IF]; Covance, Princeton, NJ; Patturajan *et al*., 1998; Komarnitsky *et al*., 2000). H5 cross-reactivities with Ser^5P peptides and phosphorylated SR proteins have been described in highly purified systems (Cho *et al*., 2001; Doyle *et al*., 2002; Licatalosi *et al*., 2002; Jones *et al*., 2004) but do not seem to contribute to the staining observed in whole cells or extracts (see *Discussion*). Other available Ser^2P antibodies available so far are not specific for pol II (CC-3; Lavoie *et al*., 1999) or also recognize Ser^5P epitopes (mara-3 and B3; Patturajan *et al*., 1998; Cho *et al*., 2001).

Primary antibodies to splicing factors were as follows: SC35 recognizes a phosphorylated epitope within the serine/arginine (SR) domain of the spliceosome assembly factor, a member of the SR family of non-small nuclear ribonucleoprotein-splicing proteins (mouse IgG1; 1:1500; Sigma Chemical; Fu and Maniatis, 1990); Sm recognizes Sm protein, a spliceosomal factor (human autoimmune antibodies; 1:2000; ANA-CDC).

Other primary antibodies were mouse anti-BrdU (1:1000; Caltag Laboratories, Burlingame, CA) and sheep anti-bromodeoxyuridine (BrdU) (1:200; BioDesign International); and rabbit anti-PSP1 (1:150; Fox *et al*., 2002). Secondary antibodies conjugated with fluorescein isothiocyanate (FITC) or Cy3 were obtained from Jackson ImmunoResearch Laboratories (West Grove, PA) (multiple labeling grade), with AlexaFluor488 or AlexaFluor555 from Molecular Probes (Eugene, OR), and with horseradish peroxidase (HRP) from Promega. For double-labeling using an IgM (H5) and an IgG (SC35; Figure 3, J and K), secondary antibodies raised in donkey against μ- or γ-immunoglobulin chains (Jackson ImmunoResearch Laboratories) were used, respectively. Control experiments in the absence of each primary antibody showed no detectable cross-reaction (our unpublished data).

Western Blotting

Total HeLa cell protein extract was prepared by harvesting HeLa cells in SDS sample buffer (10% Ficoll, 2.5 mM EDTA, 25 mM Na_3PO_4, 0.5% SDS, 0.1% bromphenol blue, 10% β-mercaptoethanol, 1 mM NaF, and 1 mM phenylmethylsulfonyl fluoride) and by passing three times through a 21-gauge needle. Denatured total protein extracts (2×10^5–3×10^5 cells/well) were separated by SDS-PAGE on 4–15% Tris-HCl gradient gels (Criterion precast gel system; Bio-Rad, Hertsfordshire, United Kingdom) and transferred to nitrocellulose membranes (Bio-Rad). Membranes were blocked (1 h) in 5% milk in Tris-buffered saline/Tween 20 (TBS-T) buffer (10 mM Tris-HCl, pH 8.0, 150 mM NaCl, and 0.05% Tween 20), incubated (2 h) in primary antibodies, washed (30 min), incubated (1 h) in HRP-conjugated secondary antibodies, and washed (30 min) all in 5% milk in TBS-T. Blots were washed in TBS-T, before detection of the HRP signal with ECL detection reagent (GE Healthcare, Little Chalfont, Buckinghamshire, United Kingdom), and exposed to Hyperfilm ECL (GE Healthcare). Scanned images were contrast stretched in Adobe Photoshop (Adobe Systems, Edinburgh, United Kingdom).

Immunofluorescence Labeling

Cryosections were rinsed (3 times) in PBS, incubated (30 min) in 20 mM glycine in PBS, rinsed (3 times) in PBS, treated (10 min) with 0.1% Triton X-100 in PBS, blocked (1 h) with PBS+ (PBS supplemented with 1% BSA, 0.2% fish skin gelatin, and 0.1% casein; pH 7.6), incubated (2 h) with primary antibodies (in PBS+), washed (3 times; 1 h) in PBS+, incubated (1 h) with secondary antibodies against mouse, rabbit, or human IgGs in PBS+, rinsed (3 times; 30 min) in PBS+, rinsed (3 times) in PBS, counterstained (45 min) with TOTO-3 (2 μM; Molecular Probes) in 0.05% Tween 20 in PBS, and rinsed successively in 0.05% Tween 20 in PBS and then PBS, before coverslips were mounted in VectaShield (Vector Laboratories, Peterborough, United Kingdom). The long incubation times used allow for antibody accessibility throughout the thickness of cryosections, providing the highest sensitivity (Branco *et al*., 2005). Negative controls included omission of primary antibodies and treatment of cryosections with alkaline phosphatase (AP) (2 h; 37°C) (0.5 U/μl, calf intestinal; New England Biolabs, Hitchin, Hertsfordshire, United Kingdom) before immunolabeling, to test the specificity of anti-pol II antibodies to phosphorylated epitopes.

Double labeling experiments were generally carried out simultaneously by combining both primary antibodies and both secondary antibodies, except when testing for the presence of pol II or Br-RNA within paraspeckles. In this case, to prevent false negative results because of antibody blocking, sections were first incubated with primary antibody against pol II or Br-RNA, washed, incubated with secondary antibody, washed (30 min) and incubated with primary antibodies anti-PSP1, and corresponding secondary antibodies.

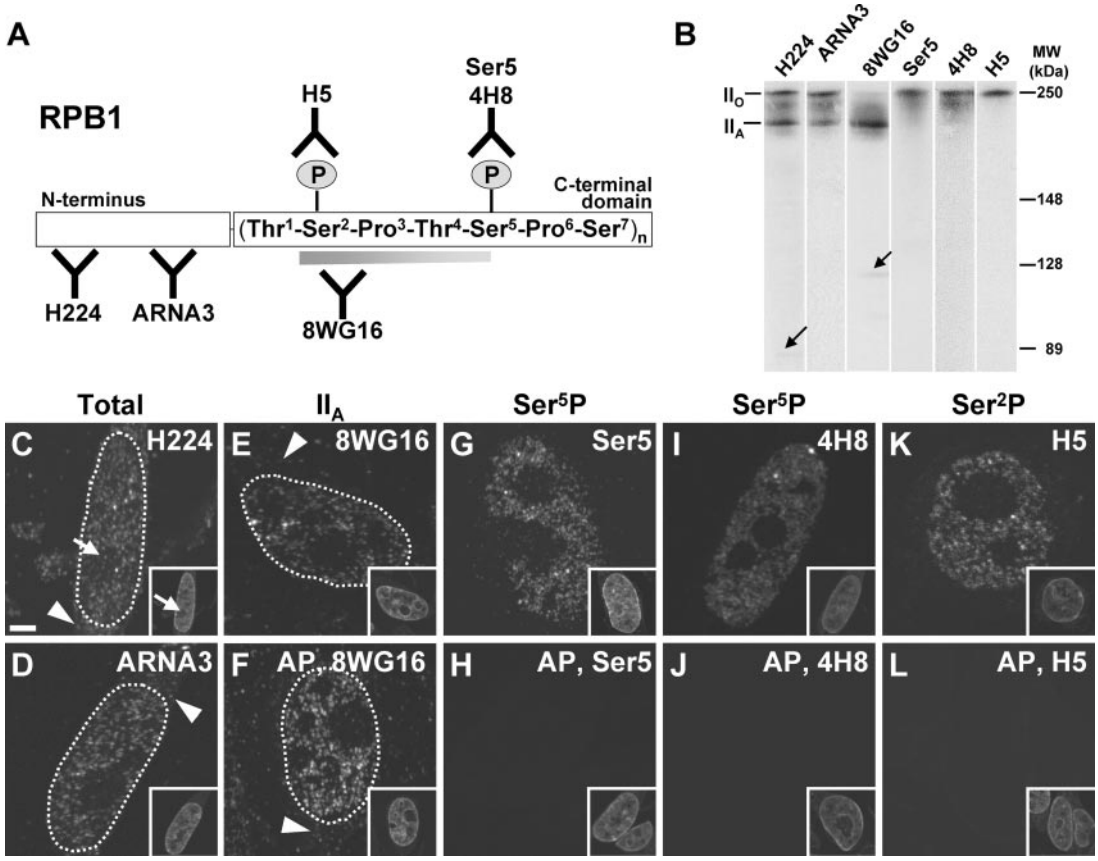

Figure 1. Characterization of antibodies against different forms of RNA polymerase II. (A) Schematic diagram for the binding sites of different antibodies against total and phosphorylated forms of the largest subunit of pol II (RPB1; *n*, number of CTD repeats). (B) Western blot analyses of HeLa whole cell extracts with antibodies against different forms of the largest subunit of pol II. Arrows indicate minor cross-reactivities. (C–L) The different forms of RPB1 are found in discrete sites throughout the nucleoplasm (dotted line), mostly outside nucleoli (arrows), with a minor fraction of unphosphorylated pol II found in the cytoplasm (arrowheads). Insets represent nucleic acid staining with TOTO-3. Total pol II was detected with antibodies H224 (C) and ARNA3 (D) against non-CTD epitopes of RPB1 in cryosections from HeLa cells. Pol II_A was detected with 8WG16 (E and F); pretreatment of sections with AP increases 8WG16 immunolabeling intensity by 1.5 times (F). Phosphorylated Ser^5 pol II was detected with rabbit anti-Ser^5P (G) and 4H8 (I) antibodies; absence of signal after pretreatment of sections with AP (H and J) shows that both antibodies bind specifically to phosphorylated epitopes. Phosphorylated Ser^2 pol II was detected with H5 (K); H5 immunolabeling signal is also sensitive to AP (L). Bar, 2 μm.

Fluorescence In Situ Hybridization to PolyA$^+$ RNA

PolyA$^+$ RNA was detected with an FITC-labeled poly(dT) probe (Sigma Chemical) in hybridization mixture (Sigma Chemical) to give 1 μM final concentration. RNA-fluorescence in situ hybridization was performed with molecular biology grade reagents (RNAse- and DNAse-free). After immunolabeling, sections were refixed (2 h) with 4% paraformaldehyde in PBS and washed (16 h) in PBS. Sections were incubated (15 min) with 2 mM vanadyl ribonucleoside complex (Sigma Chemical) in PBS (15 min), in 20 mM glycine in DEPC-treated PBS (10 min) with 0.1% Triton X-100, in DEPC-phosphate-buffered saline, and then washed (4 times) in 2× SSC. Hybridization mixture (5 μl) containing FITC-poly(dT) was denatured (10 min; 70°C), applied on Hybrislips (Molecular Probes) before covering with coverslips (10 mm in diameter) containing sections, sealed with rubber cement (Marabuwerke, Tamm, Germany), and hybridized for >60 h at 42°C. Coverslips were then washed in 2× SSC (2 times; 1 h; 20°C), in 1× SSC (2 times; 15 min), and in 0.5× SSC (15 min), and incubated (30 min) with casein blocking solution (containing 2.6% NaCl, 0.5% BSA, and 0.1% fish skin gelatin, pH 7.5–8.0; Vector Laboratories). The FITC-poly(dT) signal was amplified (2 h) with AlexaFluor488 rabbit anti-FITC (1:500; Molecular Probes), washed (3 times; 1 h), incubated (1 h) with rabbit anti-AlexaFluor488 (1:1000; Molecular Probes), washed (3 times; 1 h), and incubated (1 h) with AlexaFluor488 goat anti-rabbit (Molecular Probes), all in casein-blocking solution. Cryosections were counterstained with TOTO-3 as described above. Control experiments in the absence of poly(dT) probe in the hybridization mixture or pretreatment (1 h; 37°C) with 250 μg/ml RNAse A in 2× SSC showed no detectable signal (our unpublished data).

Microscopy

Images were acquired on a confocal laser scanning microscope (Leica TCS SP2, 100× objective, numerical aperture 1.4; Leica Camera, Milton Keynes, United Kingdom), equipped with argon (488-nm) and HeNe (543-, 633-nm) lasers, and pinhole equivalent to 1 Airy disk. Images from the different channels were collected sequentially to prevent bleedthrough. For comparison of different treatments, images were collected on the same day using the same settings, and without saturation of the intensity signal. For an unbiased representation of the whole nuclear volume, nuclear profiles were selected randomly on the TOTO-3 channel, regardless of whether sections contained splicing speckles (Supplemental Figure S2, A and C). Raw TIFF images were merged and analyzed in Adobe Photoshop (Adobe Systems) without further thresholding or filtering (e.g., no background subtraction).

Quantitative and Statistical Analyses

The quantification procedure used for splicing speckles is summarized in Supplemental Figure S2, D. Masks were drawn in the merged images, around the nucleoplasm (excluding nucleoli) in the TOTO-3 channel, around speckles in the "splicing speckle" channel, and in areas of the image outside cells (background). The areas of nucleoplasm and speckles were recorded (in pixels) for each nuclear profile in the image, and the average intensities per pixel measured within the "speckle," "nucleoplasm," and "background" masks using the Histogram function for the speckle marker (Figure 2) or pol II (Figure 3) channels.

Speckle volume was calculated as a percentage of the nucleoplasm after calculation of the percentage of nucleoplasmic area occupied by speckles (i.e.,

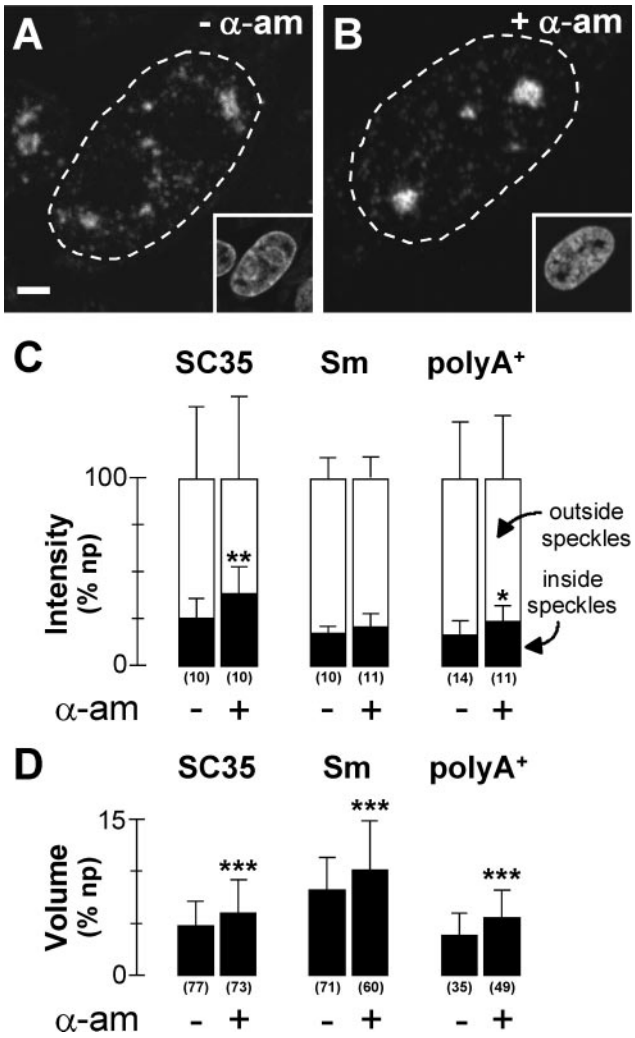

Figure 2. Effects of transcriptional inhibition on the volume of speckles and content in SC35, Sm antigen, and polyA$^+$ RNA relative to the nucleoplasm. Cryosections of HeLa cells grown in the absence (A, C, and D) or presence (B–D) of α-am were indirectly immunolabeled with antibodies against SC35 or Sm antigen, or polyA$^+$ RNA detected after in situ hybridization with a poly(dT) probe. Nuclear perimeters identified in TOTO-3 images (insets) were drawn as white dotted lines. (A) SC35 is concentrated in euchromatic domains and throughout the nucleoplasm. (B) Transcriptional inhibition by α-am causes speckles to round up and increase accumulation of SC35. Bar, 2 μm. (C and D) The np fraction of Sm antigen, SC35, or polyA$^+$ RNA present in speckles was determined after measuring the fluorescence intensity (C) and volume (D) in speckles relative to nucleoplasm in control and α-amanitin–treated cells. Total average intensity levels of SC35, Sm, and polyA$^+$ throughout the nucleoplasm did not change with α-amanitin relative to untreated samples ($p > 0.7$). α-Amanitin treatment causes statistically significant enrichment of speckle markers in speckles (except for Sm antigen; *t* test $*p \leq 0.05$ or $**p \leq 0.01$) and increase in speckle volumes (ANOVA with blocking; $***p \leq 0.003$). Numbers of nuclear profiles measured are shown in parentheses. Error bars represent standard deviations.

the ratio between area speckles and area of nucleoplasm), because the thickness of sections is significantly thinner than the size of the speckles and is equal throughout the nuclear section. Volume data were compiled from single- and double-labeling experiments, because data comparisons showed that the presence of antibodies to pol II during immunolabeling of speckles has no statistically significant effect on measurements of volume (ANOVA with blocking for different experiments; our unpublished data). The effect of α-amanitin on speckle volume was analyzed by ANOVA test with blocking (independent labeling experiments were considered as different blocks).

Average "background" intensity (per pixel) was subtracted from the intensities in the nucleoplasm and in speckles for each image. The total nucleoplasmic (np) levels of speckle markers or polymerase II was normalized relative to untreated controls (Supplemental Figure S2, D.3). For SC35, Sm, and polyA$^+$ RNA, nucleoplasmic intensities were measured in images from single-labeling experiments (Figure 2C), to avoid bias because of antibody steric hindrance detected in double-labeling experiments (our unpublished data). Results for total pol II levels represented in Figure 3 (red bars) come from double-labeling experiments but were confirmed in singly labeled cryosections (our unpublished data), with no significant differences.

The content of speckle markers or pol II in speckles was represented as a proportion of total nucleoplasmic content. For each nuclear profile, average intensities (per pixel) in the nucleoplasm and in speckles were subtracted from the image background and multiplied by the number of pixels in nucleoplasmic and speckle areas, respectively. The relative intensity present in speckles was calculated as a percentage of total intensity in the nucleoplasm and averaged for all sections analyzed (Supplemental Figure S2, D). This value represents an average for the cell population and corrects for the contribution of sections representing different regions of the nucleus. To normalize the marker content in speckles in α-amanitin–treated samples relative to untreated controls, the average content was calculated as for untreated samples, and this value was corrected with the normalized average intensity (Supplemental Figure S2, D.4).

The effects of α-amantin on total nucleoplasmic levels and on speckle content were determined using a *t* test (assumptions 2-tailed distribution and 2-sample unequal variance).

For paraspeckles, masks were drawn around the domains, before scoring for the presence of pol II or Br-RNA inside, over or outside the edge of masks. The numbers of paraspeckles analyzed ranged from 12 to 29 and originated from eight to 14 different nuclear profiles. The differences in pol II or Br-RNA localization in paraspeckles were analyzed using the chi-square statistical test after merging the values on the "edge" and "outside" speckles into one category.

RESULTS

Specificity of Pol II Antibodies and Distribution of Different Forms of Pol II in the Nucleus of HeLa Cells

The eukaryotic nucleus contains inactive and active pol II complexes that become phosphorylated on Ser^2 and Ser^5 residues at specific steps of the transcription cycle (Kobor and Greenblatt, 2002). Active complexes account for only approximately one-quarter of nuclear pol II (Jackson *et al*., 1998; Kimura *et al*., 2002), most of which is thought to be hyperphosphorylated. The presence of hyperphosphorylated forms of pol II in a nuclear compartment can be an indicator of transcriptional activity but requires confirmation by direct labeling of nascent transcripts, because not all hyperphosphorylated complexes in the cell are associated with DNA (Warren *et al*., 1992; Jackson *et al*., 1998; Kimura *et al*., 2002). Conversely, the presence of hypophosphorylated pol II in a compartment may suggest a role in storage of inactive pol II complexes or could simply reflect some level of permeability. A role in storage can be put in evidence by changing the equilibrium between active and inactive complexes, for example, after transcription inhibition with the drug α-amanitin (Carmo-Fonseca *et al*., 1992; Spector *et al*., 1993).

We first tested the specificity of antibodies that recognize different forms of the largest subunit of pol II, RPB1, in Western blots and their labeling properties in fixed HeLa cells (Figure 1; see *Materials and Methods* and supplemental material for a detailed description of the properties of each antibody). Six antibodies were highly specific for RPB1 in Western blots, three antibodies with specificity for phosphorylated epitopes showed full sensitivity to AP, and all gave consistent results by in situ immunofluorescence.

SDS-PAGE separates RPB1 molecules into two main bands, II_A and II_O, which correspond to hypo- and hyperphosphorylated forms of the subunit, respectively, and an intermediate smear with increasing levels of phosphorylation (Figure 1B). Total pol II can be recognized by antibodies H224 and ARNA3, which bind to non-CTD domains of RPB1 and therefore label

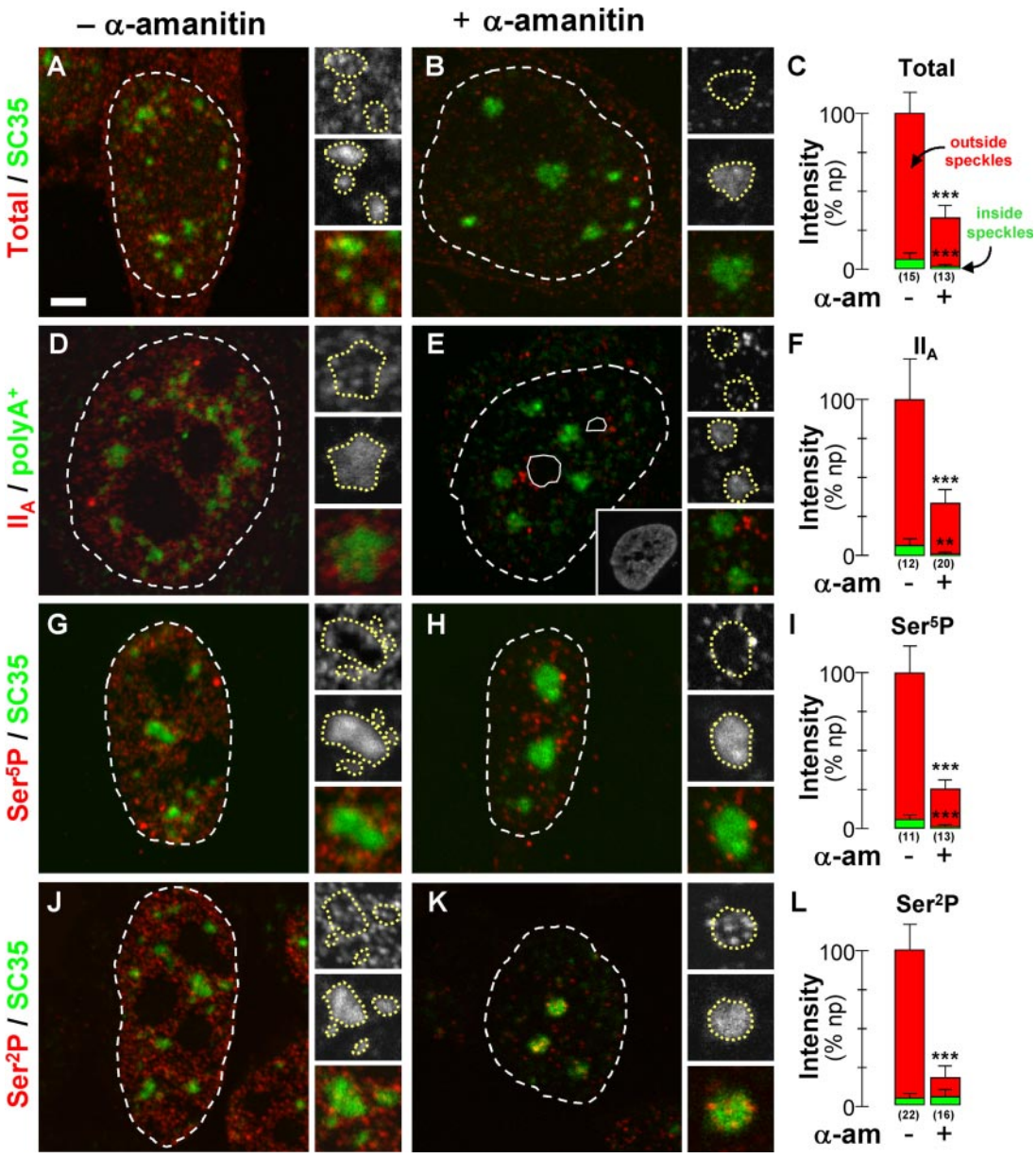

Figure 3. RNA polymerase II is not recruited to splicing speckles upon transcriptional inhibition. Cryosections of HeLa cells grown in the absence (A, D, G, and J) or presence (B, E, H, and K) of α-am were indirectly immunolabeled with antibodies against different forms of pol II and splicing speckle markers (SC35 or polyA$^+$ RNA). Nuclear perimeters were identified in the TOTO-3 images and drawn as white dotted lines or shown as an inset. Higher magnification images of speckles are shown on the right-hand side of lower magnification images. Bar, 2 μm. The np fraction of pol II present in speckles is a ratio of total fluorescence intensity in speckles relative to total intensity throughout the nucleoplasm (C, F, I, and L). The effects α-amanitin on the total amounts of pol II in the nucleoplasm or in speckles are statistically significant except for the amount of Ser^{2}P pol II (L) in speckles, which remains constant (*t* test; **p ≤ 0.01 or ***p ≤ 0.001); numbers of nuclear profiles measured are shown in parentheses). Error bars represent standard deviations. (A–C) Total pol II (H224; red) and SC35 (green) in control (A) and α-amanitin–treated (B) cells. A small fraction of total pol II is found in speckles; upon transcriptional inhibition, total pol II levels decrease proportionally in both np and speckles (C). (D–F) Pol II$_A$ (8WG16; red) and polyA$^+$ RNA (green). A small fraction of pol II$_A$ is found within speckles; upon transcriptional inhibition, levels decrease in nucleoplasm and speckles (F), and a small number of brighter II$_A$ sites are seen around nucleoli (E; solid line). (G–I) Phosphorylated Ser^5 pol II (rabbit anti-Ser^{5}P; red) and SC35 (green). A small fraction of phospho-Ser^5 pol II is found in speckles, mostly at their periphery; upon transcriptional inhibition, levels decrease in both nucleoplasm and speckles (I). (J–L) Phosphorylated Ser^2 pol II (H5; red) and SC35 (green). A small fraction of phospho-Ser^2 pol II is found in speckles; upon transcriptional inhibition, levels decrease throughout the nucleoplasm, whereas levels within speckles remain constant (L).

both pol II$_A$ and II$_O$ bands in Western blots of whole HeLa cell extracts (Figure 1, A and B). The II$_A$ form can be detected with antibody 8WG16 raised against unphosphorylated CTD (Figure 1B), which also detects a minor fraction of slower migrating molecules, but little of the II$_O$ band (Figure 1B). For simplicity, hereafter, we refer to the pol II molecules detected by 8WG16 as pol II$_A$. Pol II forms phosphorylated on Ser^5 can be detected with rabbit anti-Ser^{5}P and 4H8 antibodies; both antibodies

label the II_O form and a smear of faster migrating forms, but not the II_A band (Figure 1B). Pol II complexes phosphorylated on Ser^2 can be detected with antibody H5 (Patturajan *et al.*, 1998), which exclusively detects the II_O band in whole cell extracts, but not the II_A form or the intermediate smear, which is detected by antibodies to Ser^{5}P (Figure 1B; see *Discussion* for comments on previously described cross-reactions of H5). These results suggest that most "hypophosphorylated" II_A molecules have little phosphorylation on Ser^2 or Ser^5 residues.

To characterize the in situ labeling patterns of each antibody in HeLa cells, we used ultrathin cryosections (100–150 nm in thickness) of sucrose-embedded cells because they maximize antibody accessibility to nuclei fixed under conditions that preserve ultrastructure (Figure S2, B; Guillot *et al.*, 2004; Branco *et al.*, 2005), and they also improve the axial resolution of confocal microscopes (Pombo *et al.*, 1999a). All pol II forms studied here are found in discrete sites outside nucleoli, with a small number of brighter sites observed in some nuclear sections (Figure 1, C–G, I, and K; note that ~150-nm-thick cryosections correspond to ~1/50 of a nucleus with 5- to 10-μm diameter). EGFP-RPB1 and other subunits of pol II show similar distributions (Jones *et al.*, 2000; Sugaya *et al.*, 2000). Antibodies against the N terminus or nonphosphorylated CTD also detect pol II in the cytoplasm, where RPB1 is likely to be translated (Figure 1, C–F, arrowheads). All detectable immunoreactivity of antibodies to Ser^{5}P or Ser^{2}P pol II is sensitive to AP (Figure 1, H, J, and L). Although all pol II forms have a homogeneous distribution in the nucleus of HeLa cells, without obvious concentration in speckles, it remained possible that some forms of pol II are specifically stored in these compartments.

Inhibition of Transcriptional Activity Induces Minor Changes in the Volume and Splicing Factor Enrichment of "Splicing Speckles"

To ask whether splicing speckles act as storage sites of pol II, we first characterized speckles in our imaging conditions in control and α-amanitin–treated cells to reveal the extent of recruitment because of transcriptional inhibition (Figure 2). Comparisons of three markers of speckles, Sm antigen, SC35, and polyA$^+$ RNA, show they colocalize in large interchromatin domains, as expected (Supplemental Figure S1). As shown previously, splicing speckles become more prominent after α-amanitin treatment (Figure 2, A and B; Carmo-Fonseca *et al.*, 1992; Spector *et al.*, 1993). To compare the amount of splicing factors and polyA$^+$ RNA concentrated in speckles relative to the nucleoplasm in control and α-amanitin–treated cells, we developed a simple stereological procedure that involves computing the proportion of intensity signal contained in speckles relative to the total signal present throughout the nucleoplasm (see *Materials and Methods* and Supplemental Figure S2). Speckles contain approximately one-fifth of the nucleoplasm content in SC35, Sm antigen, and polyA$^+$ RNA (25, 18, and 17%, respectively; Figure 2C; see also Fay *et al.*, 1997; Wei *et al.*, 1999). The total volume occupied by speckles is relatively small (5, 8, and 4% of the nucleoplasm for speckles marked by SC35, Sm antigen, and polyA$^+$ RNA, respectively; Figure 2D), showing that the splicing factor and polyA$^+$ enrichment in speckles is only two- to fourfold relative to the whole nucleoplasm. The small differences between speckle markers are likely to reflect difficulties with identifying smaller speckles with SC35 and polyA$^+$ RNA, which give more discrete patterns.

After α-amanitin treatment in vivo, speckles round up and seem more enriched in SC35 (Figure 2, A and B; Spector *et al.*, 1993). Unlike what might be predicted from visual inspection of images, intensity measurements show that the recruitment of SC35 into splicing speckles after transcriptional inhibition is relatively small (increasing from 25 to 39% of total nucleoplasmic intensity after treatment with α-amanitin), but statistically highly significant (*t* test; $p = 0.01$). Only a marginal, but statistically significant increase, is observed for polyA$^+$ RNA, with no significant effect detected in the case of Sm antigen (Figure 2C). The volume of speckles increases slightly to 6, 10, and 6% of the nucleoplasm volume for SC35, Sm antigen, and polyA$^+$, respectively (Figure 2D); the increase in volume relative to untreated cells for the three speckle markers is statistically highly significant (ANOVA test; $p \leq 0.003$).

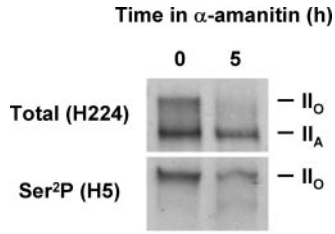

Figure 4. Western blot analyses confirm reduction pol II levels after treatment with α-amanitin. HeLa cells were grown ± 50 μg/ml α-amanitin for 5 h, before whole cell extracts were prepared and analyzed by Western blot with antibodies against total pol II (H224) and Ser^{2}P pol II (H5). Western with H224 reveals a decrease in the levels of hyperphosphorylated (II_O band) and hypophosphorylated (II_A band) forms of pol II. Western blots with H5 confirm a marked reduction in the levels of Ser^{2}P pol II.

Splicing Speckles Contain but Are Not Enriched in Any of the Different Phosphorylated Forms of Pol II

We next tested whether any of the different pol II forms are present in splicing speckles, using SC35 or polyA$^+$ RNA as markers, depending on the origin of the pol II antibodies available (Figure 3; analyses using Sm antigen gave similar results; our unpublished data). All forms of pol II are found within speckles (Figure 3, A, D, G, and J) but in relative amounts that are proportional to speckle volume (7, 7, 6, and 4% for total pol II, II_A, Ser^{5}P, and Ser^{2}P, respectively; Figure 3, C, F, I, and L), indicating that pol II is neither enriched nor depleted in speckles relative to the whole nucleoplasm. Biochemical purification of speckles is consistent with this result, because pol II copurifies with splicing speckles, but no enrichment is detected relative to whole nuclear extracts (Mintz *et al.*, 1999).

Splicing Speckles Do Not Act as Nuclear Reservoirs of Pol II but Contain a Small Pool of Stably Bound Ser^{2}P Pol II

To reveal whether splicing speckles act as nuclear reservoirs of inactive pol II complexes, we inhibited pol II activity with α-amanitin and measured whether the speckle content in pol II increased. Cryosections from cells grown in the absence or presence of α-amanitin were immunolabeled in parallel and imaged under the same, nonsaturating conditions. After α-amanitin treatment, the total nucleoplasmic levels of total pol II, pol II_A, and Ser^{5}P pol II decrease to 33, 34, and 26%, respectively, relative to untreated cells (Figure 3, A–I). The levels within speckles also decrease to approximately one-third (from ~6 to 7 to ~1 to 2%), implying that pol II complexes in speckles are not stably bound but in transit through these domains. The reduction in total pol II levels was confirmed by Western blot analyses for total pol II (Figure 4). Previous analyses of pol II levels by Western blotting also show a decrease in pol II levels induced by α-amanitin (Bregman *et al.*, 1995; Nguyen *et al.*,

1996). Although Nguyen *et al*. (1996) reported complete degradation of pol II after 4 h in 100 μg/ml α-amanitin (or 24 h in 20 μg/ml), our results are consistent with those of Bregman *et al*. (1995) in which some Ser[5]P pol II is detected after 8 h in 10 μg/ml α-amanitin (and after 3 h in 100 μM 5,6-dichloro-1-β-D-ribofuranosylbenzimidazole [DRB]). Such discrepancies are likely to result from differences in sensitivity of Western blotting protocols used in the different laboratories. We also confirmed the presence of pol II and reduction in levels after α-amanitin treatment on equatorial optical sections from whole cells after immunolabeling with the same panel of antibodies (Guillot, Martin, Antunes, Bentley, and Pombo, unpublished data; also see Bregman *et al*., 1995). Alternative inhibitors of pol II activity, such as DRB, also cause a reduction, albeit less pronounced, of pol II levels in the nucleoplasm, and do not cause detectable accumulation of pol II forms detected with antibodies against total pol II in speckles (Guillot and Pombo, unpublished data; also see Bregman *et al*., 1995). However, one study claims that DRB has no effect on pol II levels (Nguyen *et al*., 1996).

Careful analysis of pol II_A distribution in α-amanitin–treated cells also revealed the presence of a small number of intensely labeled sites containing this form of pol II around nucleoli (Figure 3E, solid line; also see Figure 6D), reminiscent of perinucleolar caps such as those seen with coilin, fibrillarin, or paraspeckle protein (Fox *et al*., 2002; Ospina and Matera, 2002). The perinucleolar pol II_A sites detected by 8WG16 do not colocalize with polyA$^+$ RNA (Figure 3E), coilin, or fibrillarin (our unpublished data), but they do colocalize with paraspeckle protein (see below).

In contrast to the other forms of pol II, the amount of Ser[2]P pol II in speckles remained constant (~5% of nucleoplasmic intensity) after α-amanitin treatment, whereas the reduction detected in the nucleoplasm was more prominent (to ~18% relative to untreated cells; Figure 3, J–L; also confirmed by Western blot, Figure 4, and by immunofluorescence analysis of whole cells; Guillot and Pombo, unpublished data). Although visual inspection of images has previously suggested that Ser[2]P pol II is recruited from the nucleoplasm to speckles upon transcriptional inhibition (Bregman *et al*., 1995; Mintz and Spector, 2000), the intensity measurements presented here dismiss this conclusion. The general decrease in Ser[2] phosphorylation in euchromatic areas is expected as phosphorylation on Ser[2] correlates with transcription elongation, which is inhibited within 1 h of the α-amanitin treatment used here (measured after Br-UTP incorporation; our unpublished data). The lack of sensitivity to α-amanitin and the absence of little detectable chromatin in splicing speckles suggest that the pol II molecules present in speckles are not engaged in transcription. The use of other inhibitors of pol II activity, such as DRB, also revealed a stable pool of Ser[2]P pol II in speckles (Guillot and Pombo, unpublished; also see Bregman *et al*., 1995).

To confirm that Ser[2]P pol II complexes present in speckles are transcriptionally inactive, we localized sites of transcription relative to speckles after incorporation of Br-UTP into newly made RNA. We labeled nascent RNAs in cells permeabilized with a mild detergent in conditions that preserve cellular ultrastructure and the activity of all three nuclear polymerases (I, II, and III), while preventing any detectable movement of completed RNAs down the transport pathway (Iborra *et al*., 1996; Pombo *et al*., 1999b). Br-RNA was detected at the edges of speckles (Figure 5; Puvion and Puvion-Dutilleul, 1996; Iborra *et al*., 1998; Cmarko *et al*., 1999), unlike what is observed for Ser[2]P pol II (Figure 3K).

The presence of Br-RNA at the periphery of speckles is consistent with identification of active genes in this region.

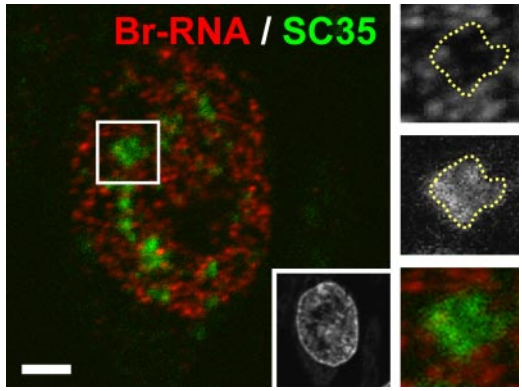

Figure 5. Splicing speckles are not transcriptionally active. Newly labeled Br-RNA (red) was found over the edges of, but not within splicing speckles marked by SC35 (green). Higher magnification view of speckle inside white box is shown on the right hand side. Bar, 2 μm.

Although previous analyses of whole cells reported 15–45% of Br-RNA signal in the nucleoplasm is present within nuclear speckles (Fay *et al*., 1997; Wei *et al*., 1999), our higher resolution approach finds only ~5% of Br-RNA at the edge of speckles (marked by SC35 or polyA$^+$ RNA).

Paraspeckles Contain Pol II_A but Little Ser[2]P Form or Newly Made Br-RNA

We next investigated whether the splicing-associated, paraspeckle domains contained pol II or could be involved in the transcriptional events that take place at the speckle periphery. Because paraspeckles are too small to act as main reservoirs of pol II, we scored the number of parapeckles that contained pol II (Figure 6), instead of measuring the relative content of pol II. Total pol II marked by non-CTD antibodies is found within most paraspeckles (77%) or at their periphery (23%; Figure 6, A and G). The presence of pol II within these domains was confirmed with antibody 8WG16 to hypophosphorylated forms (with or without pretreatment with AP to remove phospho groups; Figure 6, B and G); 8WG16 labels 95% of paraspeckles, probably because of the increased sensitivity afforded by the detection of multiple heptad repeats in the CTD.

Because paraspeckles relocate to the periphery of the nucleolus after transcriptional inhibition with actinomycin D and DRB (Fox *et al*., 2002, 2005), in the form of cap structures such as those observed here for pol II_A after α-amanitin treatment (Figure 2E), we investigated whether pol II remained stably associated with paraspeckles in these conditions. We found pol II_A colocalized in the same nucleolar caps as PSP1 (Figure 6D), but not coilin (our unpublished data), indicating that the association between nonphosphorylated pol II and PSP1 in paraspeckles is likely to be stable (Figure 6D).

Ser[5]P and Ser[2]P pol II were both found within paraspeckles but only in 31 and 11% of the domains, respectively (Figure 6, C, E, and G); most of the remaining paraspeckles were surrounded by these forms of pol II. To test whether the pol II complexes present within paraspeckles are transcriptionally active, we labeled nascent transcripts after incorporation of Br-UTP. Most paraspeckles do not contain but are surrounded by Br-RNA (Figure 5, F and G; Fox *et al*., 2002). These results indicate that although paraspeckles may be involved in pol II metabolism, they are unlikely to be sites of transcription. Chi-square statistical test showed that differences in the frequency of colocalization of pol II forms or Br-RNA within paraspeckles

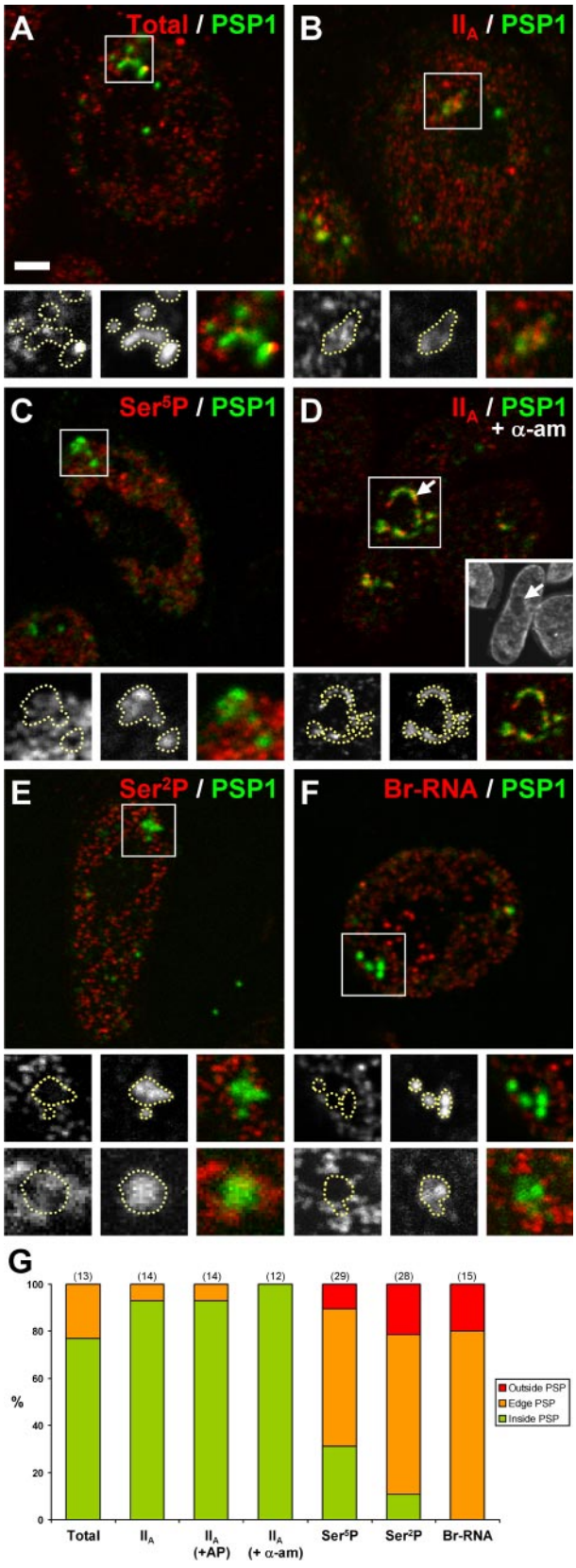

Figure 6. Paraspeckles are not transcriptionally active but contain pol II. Paraspeckles contain total pol II (A; detected with ARNA-3), pol II_A (B; detected with 8WG16), and Ser^5P pol II (C; detected with 4H8). Higher magnification views of paraspeckles inside white box are shown below each low-power image. Pol II_A colocalizes in PSP1 nucleolar caps formed after α-am treatment (arrow in D). Little detectable Ser^2P pol II or Br-RNA is found within paraspeckles (E and F). The magnified views in the last row show two additional examples of paraspeckle domains in which Ser^2P or Br-RNA were found inside or at the edge of paraspeckles, respectively. Bar, 2 μm. (G) Quantitative analysis of the number of paraspeckles containing pol II or Br-RNA outside (red), at the edge of (orange), or inside (green) the domains. Numbers of paraspeckles analyzed are shown in parentheses. The chi-square statistical test was performed after merging the values on the "edge" and "outside" speckles into one category; differences were found to be highly significant ($p < 0.0001$).

are highly significant ($p < 0.0001$). The differences in localization between Ser^5P and Ser^2P forms and Br-RNA also indicate that the presence of phosphorylated forms of pol II within a nuclear domain does not necessarily imply that the domain is transcriptionally active, as seen previously for Cajal bodies (Schul *et al.*, 1998; Xie and Pombo, 2005).

DISCUSSION

RNA Polymerase II Is Present but Not Enriched within Splicing Speckles

Splicing speckles are major nuclear domains that occupy 5–10% of the nucleoplasmic volume and are enriched in splicing factors and $polyA^+$ RNA by a factor of 2 to 4 relative to the nucleoplasm (Figure 2; Fay *et al.*, 1997; Wei *et al.*, 1999). We find that all forms of pol II studied here are present in splicing speckles (Figure 3), but in contrast with previous reports, we do not detect an enrichment of Ser^2P pol II, nor of any other pol II form, in these ultrastructurally preserved samples (Bregman *et al.*, 1995; Mintz and Spector, 2000; Guillot *et al.*, 2004). A small pool of hyperphosphorylated pol II is also detected in speckles after biochemical purification of these compartments (Mintz *et al.*, 1999).

Transcription Occurs at the Edge of but Not within Splicing Speckles

Here, we confirm that the interior of speckles is transcriptionally inactive, because little nucleotide incorporation into RNA is detected (also see Puvion and Puvion-Dutilleul, 1996; Iborra *et al.*, 1998; Cmarko *et al.*, 1999). However, a growing number of genes have been found associated with speckles (Shopland *et al.*, 2003; Moen *et al.*, 2004). The resolution of confocal microscopes is limited by the diffraction of light; on the *z*-axis, it is at best 500 nm and in the size range of most speckles. As suggested from the three- to ninefold overestimation of transcriptional activity in speckles after whole cell measurements of Br-RNA (Fay *et al.*, 1997; Wei *et al.*, 1999) relative to higher resolution achieved after the use of ultrathin sections (Figure 5; Puvion and Puvion-Dutilleul, 1996; Iborra *et al.*, 1998; Cmarko *et al.*, 1999), some of the associations detected between specific genes and speckles in confocal micrographs of whole cells are likely to be too distant to be biologically meaningful. Nevertheless, the accumulation of transcripts in speckles and their enrichment after splice-site mutation provides compelling evidence that some pre-mRNAs cycle through speckles to complete splicing or as a quality control mechanism for unprocessable transcripts (Johnson *et al.*, 2000). Transient association of $polyA^+$ RNAs with speckles has also been recently observed in vivo using fluorescent 2′-*O*-methyl oligoribonucleotide probes (Molenaar *et al.*, 2004).

Inhibition of Transcription Does Not Result in Pol II Recruitment to Speckles but Reveals a Stably Bound Pool of Ser^{2}P Pol II Complexes

Because the nuclear dynamics of phosphorylated forms cannot so far be assessed by live cell imaging, we set out to analyze the stability of pol II association with speckles after inhibition of pol II transcription. If speckles were storage sites for RNA pol II, transcriptional inhibition should result in an enrichment of pol II in these domains. We find the opposite is true (Figure 3); total pol II levels throughout the nucleoplasm and within speckles decrease proportionally, arguing against a function of splicing speckles as a pool of inactive pol II complexes. These results are consistent with the "sponge-like" properties of splicing speckles recently characterized in the *Xenopus* oocyte nucleus (Handwerger *et al*., 2005), and with the idea that pol II complexes cruise through these permeable nuclear compartments.

The hyperphosphorylated Ser^{2}P pol II showed a different behavior. Although no enrichment was detected, the levels of Ser^{2}P pol II complexes in speckles remained constant after transcriptional inhibition, whereas levels in the nucleoplasm were greatly diminished. This suggests that Ser^{2}P complexes in speckles represent a stable component of these domains that do not freely exchange with the nucleoplasm.

Cross-reactivity of H5 with Ser^{5}P CTD peptides and phosphorylated SR proteins has been identified in highly purified systems (Cho *et al*., 2001; Doyle *et al*., 2002; Licatalosi *et al*., 2002; Jones *et al*., 2004). However, a number of arguments indicate that these cross-reactivities have little contribution to the staining detected in situ after immunofluorescence. First, Ser^{5}P pol II is significantly reduced in speckles after α-amanitin, unlike the epitope detected by H5, which remains constant (Figure 3). Second, H5 does not bind to Cajal bodies, although these domains are rich in the Ser^{5}P form (Schul *et al*., 1998; Doyle *et al*., 2002; Xie and Pombo, 2005). It is more difficult to rule out that some of the H5 staining in speckles is because of cross-reactivity to hyperphosphorylated SR proteins. However, it is generally thought that hyperphosphorylated SR proteins reside outside speckles (Gui *et al*., 1994; Colwill *et al*., 1996; Neugebauer and Roth, 1997). Finally, the presence of hyperphosphorylated RPB1 and other pol II subunits in speckles is also detected by mass spectrometry after biochemical purification of these compartments (Mintz *et al*., 1999).

Because phosphorylated pol II is required for splicing (Hirose *et al*., 1999) and promotes assembly of spliceosomes (Zeng and Berget, 2000), an intriguing possibility for the role of Ser^{2}P pol II in speckles is that the CTD may serve as a platform for posttranscriptional splicing of long transcripts known to traffic through speckles and accumulate in these domains when they contain a splice-site mutation (Johnson *et al*., 2000). Although CTD truncation has no effect on splicing of injected β-globin pre-mRNA in *Xenopus* oocytes (Bird *et al*., 2004), it remains possible that the specific pre-mRNAs found to accumulate in speckles in mammalian cells require a phosphorylated CTD for posttranscriptional splicing. Because splicing speckles are present in cells that contain a CTD-truncated RPB1, the CTD itself is unlikely to be a structural component of these domains (Misteli and Spector, 1999). Three other arguments show that Ser^{2}P modification is not exclusively associated with transcriptionally active complexes and may have roles other than in transcription. First, Ser^{2}P complexes are present in mitotic cells when pol II is inactive (Bregman *et al*., 1994), with potential roles in inactivation of transcription initiation and splicing factor recruiting to the nucleus upon nuclear envelope formation. Second, ~10% of Ser^{2}P pol II in the cell is not resistant to treatment with the detergent sarkosyl and therefore is probably transcriptionally inactive (Jackson *et al*., 1998). Third, Ser^{2}P complexes within speckles are insensitive to α-amanitin (Figure 3K) and DRB (Bregman *et al*., 1995).

Paraspeckles Are Not Sites of Transcription but Are Stably Associated with Pol II$_A$

Paraspeckles are marked by PSP1 and PSP2 proteins, which interact with CTD-binding proteins, such as p54nrb and PSF, and are found at the periphery of splicing speckles (Emili *et al*., 2002; Fox *et al*., 2002, 2005; Kameoka *et al*., 2004; Myojin *et al*., 2004), where active genes are also associated. We tested whether paraspeckles contain pol II or are sites of transcription and found that they contain the Ser^{5}P form of pol II but little of the Ser^{2}P form or newly made Br-RNA (Figure 6). Furthermore, upon transcriptional inhibition, pol II and p54nrb remain stably bound to paraspeckles when they relocate to the periphery of nucleoli (Figure 6D; Fox *et al*., 2005). The presence of pol II in paraspeckles and the cycling of these compartments between splicing speckles and nucleoli suggests a role in pol II recycling, but it remains unclear why some pol II complexes would be transported to and from the periphery of nucleoli.

In summary, our results show that splicing speckles and paraspeckles are likely to be involved in pol II metabolism but are not major sites of gene transcription or polymerase II storage. It remains to be determined whether the Ser^{2}P pol II complexes present in speckles are required for posttranscriptional splicing that may occur in these domains.

ACKNOWLEDGMENTS

We thank Drs. Archa Fox and Angus Lamond for PSP1 antibodies; Dr. André Möller, Julie K. Stock, and Miguel R. Branco for comments on the manuscript; Dr. Francisco Ramirez for performing the ANOVA analysis; and the Medical Research Council (United Kingdom) for support (to S.Q.X., S. M., P.V.G., and A. P.). D.L.B. is supported by National Institutes of Health Grant GM-063873.

REFERENCES

Bird, G., Zorio, D.A.R., and Bentley, D. L. (2004). RNA polymerase II carboxy-terminal domain phosphorylation is required for cotranscriptional pre-mRNA splicing and 3′-end formation. Mol. Cell. Biol. *24*, 8963–8969.

Bisotto, S., Lauriault, P., Duval, M., and Vincent, M. (1995). Colocalization of a high molecular mass phosphoprotein of the nuclear matrix (p255) with spliceosomes. J. Cell Sci. *108*, 1873–1882.

Branco, M. R., Xie, S. Q., Martin, S., and Pombo, A. (2005). Correlative microscopy using Tokuyasu cryosections: applications for immunolabeling and in situ hybridization. In: Cell Imaging, ed. D. Stephens: Scion Publishing, 201–217.

Bregman, D. B., Du, L., Li, Y., Ribisi, S., and Warren, S. L. (1994). Cytostellin distributes to nuclear regions enriched with splicing factors. J. Cell Sci. *107*, 387–396.

Bregman, D. B., Du, L., Van Der Zee, S., and Warren, S. L. (1995). Transcription-dependent redistribution of the large subunit of RNA polymerase II to discrete nuclear domains. J. Cell Biol. *129*, 287–298.

Carmo-Fonseca, M., Pepperkok, R., Carvalho, M. T., and Lamond, A. I. (1992). Transcription-dependent colocalization of the U1, U2, U4/U6, and U5 snRNPs in coiled bodies. J. Cell Biol. *117*, 1–14.

Cho, E. J., Kobor, M. S., Kim, M., Greenblatt, J., and Buratowski, S. (2001). Opposing effects of Ctk1 kinase and Fcp1 phosphatase at Ser 2 of the RNA polymerase II C-terminal domain. Genes Dev. *15*, 3319–3329.

Clemson, C. M., and Lawrence, J. B. (1996). Multifunctional compartments in the nucleus: insights from DNA and RNA localization. J. Cell. Biochem. *62*, 181–190.

Cmarko, D., Verschure, P. J., Martin, T. E., Dahmus, M. E., Krause, S., Fu, X. D., van Driel, R., and Fakan, S. (1999). Ultrastructural analysis of transcription and splicing in the cell nucleus after bromo-UTP microinjection. Mol. Biol. Cell *10*, 211–223.

Colwill, K., Pawson, T., Andrews, B., Prasad, J., Manley, J. L., Bell, J. C., and Duncan, P. I. (1996). The Clk/Sty protein kinase phosphorylates SR splicing factors and regulates their intranuclear distribution. EMBO J. *15*, 265–275.

Doyle, O., Corden, J. L., Murphy, C., and Gall, J. G. (2002). The distribution of RNA polymerase II largest subunit (RPB1) in the *Xenopus* germinal vesicle. J. Struct. Biol. *140*, 154–166.

Emili, A., Shales, M., McCracken, S., Xie, W., Tucker, P. W., Kobayashi, R., Blencowe, B. J., and Ingles, C. J. (2002). Splicing and transcription-associated proteins PSF and p54nrb/nonO bind to the RNA polymerase II CTD. RNA *8*, 1102–1111.

Fay, F. S., Taneja, K. L., Shenoy, S., Lifshitz, L., and Singer, R. H. (1997). Quantitative digital analysis of diffuse and concentrated nuclear distributions of nascent transcripts, SC35 and poly(A). Exp. Cell Res. *231*, 27–37.

Fox, A. H., Bond, C. S., and Lamond, A. I. (2005). P54nrb forms a heterodimer with PSP1 that localizes to paraspeckles in a RNA-dependent manner. Mol. Biol. Cell *16*, 4304–5315.

Fox, A. H., Lam, Y. W., Leung, A. K., Lyon, C. E., Andersen, J., Mann, M., and Lamond, A. I. (2002). Paraspeckles. A novel nuclear domain. Curr. Biol. *12*, 13–25.

Fu, X. D., and Maniatis, T. (1990). Factor required for mammalian spliceosome assembly is localized to discrete regions in the nucleus. Nature *343*, 437–441.

Grande, M. A., van der Kraan, I., de Jong, L., and van Driel, R. (1997). Nuclear distribution of transcription factors in relation to sites of transcription and RNA polymerase II. J. Cell Sci. *110*, 1781–1791.

Gui, J. F., Lane, W. S., and Fu, X. D. (1994). A serine kinase regulates intracellular localization of splicing factors in the cell cycle. Nature *369*, 678–682.

Guillot, P. V., Xie, S. Q., Hollinshead, M., and Pombo, A. (2004). Fixation-induced redistribution of hyperphosphorylated RNA polymerase II in the nucleus of human cells. Exp. Cell Res. *295*, 460–468.

Handwerger, K. E., Cordero, J. A., and Gall, J. G. (2005). Cajal bodies, nucleoli, and speckles in the *Xenopus* oocyte nucleus have a low-density, sponge-like structure. Mol. Biol. Cell *16*, 202–211.

Herrmann, C. H., and Mancini, M. A. (2001). The Cdk9 and cyclin T subunits of TAK/P-TEFb localize to splicing factor-rich nuclear speckle regions. J. Cell Sci. *114*, 1491–1503.

Hirose, Y., Tacke, R., and Manley, J. L. (1999). Phosphorylated RNA polymerase II stimulates pre-mRNA splicing. Genes Dev. *13*, 1234–1239.

Iborra, F. J., Jackson, D. A., and Cook, P. R. (1998). The path of transcripts from extra-nucleolar synthetic sites to nuclear pores: transcripts in transit are concentrated in discrete structures containing SR proteins. J. Cell Sci. *111*, 2269–2282.

Iborra, F. J., Pombo, A., Jackson, D. A., and Cook, P. R. (1996). Active RNA polymerases are localized within discrete transcription "factories'in human nuclei. J. Cell Sci. *109*, 1427–1436.

Jackson, D. A., Iborra, F. J., Manders, E. M., and Cook, P. R. (1998). Numbers and organization of RNA polymerases, nascent transcripts, and transcription units in HeLa nuclei. Mol. Biol. Cell *9*, 1523–1536.

Johnson, C., Primorac, D., McKinstry, M., McNeil, J., Rowe, D., and Lawrence, J. B. (2000). Tracking COL1A1 RNA in osteogenesis imperfecta: splice-defective transcripts initiate transport from the gene but are retained within the SC35 domain. J. Cell Biol. *150*, 417–432.

Jones, E., Kimura, H., Vigneron, M., Wang, Z., Roeder, R. G., and Cook, P. R. (2000). Isolation and characterization of monoclonal antibodies directed against subunits of human RNA polymerases I, II, and III. Exp. Cell Res. *254*, 163–172.

Jones, J. C., Phatnani, H. P., Haystead, T. A., MacDonald, J. A., Alam, S. M., and Greenleaf, A. L. (2004). C-terminal repeat domain kinase I phosphorylates Ser2 and Ser5 of RNA polymerase II C-terminal domain repeats. J. Biol. Chem. *279*, 24957–24964.

Kameoka, S., Duque, P., and Konarska, M. M. (2004). p54(nrb) associates with the 5′ splice site within large transcription/splicing complexes. EMBO J. *23*, 1782–1791.

Kimura, H., Sugaya, K., and Cook, P. R. (2002). The transcription cycle of RNA polymerase II in living cells. J. Cell Biol. *159*, 777–782.

Kobor, M. S., and Greenblatt, J. (2002). Regulation of transcription elongation by phosphorylation. Biochim. Biophys. Acta *1577*, 261–275.

Komarnitsky, P., Cho, E. J., and Buratowski, S. (2000). Different phosphorylated forms of RNA polymerase II and associated mRNA processing factors during transcription. Genes Dev. *14*, 2452–2460.

Kruhlak, M. J., Lever, M. A., Fischle, W., Verdin, E., Bazett-Jones, D. P., and Hendzel, M. J. (2000). Reduced mobility of the alternate splicing factor (ASF) through the nucleoplasm and steady state speckle compartments. J. Cell Biol. *150*, 41–51.

Lamond, A. I., and Spector, D. L. (2003). Nuclear speckles: a model for nuclear organelles. Nat. Rev. Mol. Cell. Biol. *4*, 605–612.

Lavoie, S. B., Albert, A. L., Thibodeau, A., and Vincent, M. (1999). Heat shock-induced alterations in phosphorylation of the largest subunit of RNA polymerase II as revealed by monoclonal antibodies CC-3 and MPM-2. Biochem. Cell Biol. *77*, 367–374.

Licatalosi, D. D., Geiger, G., Minet, M., Schroeder, S., Cilli, K., McNeil, J. B., and Bentley, D. L. (2002). Functional interaction of yeast pre-mRNA 3′ end processing factors with RNA polymerase II. Mol. Cell *9*, 1101–1111.

Maniatis, T., and Reed, R. (2002). An extensive network of coupling among gene expression machines. Nature *416*, 499–506.

Mintz, P. J., Patterson, S. D., Neuwald, A. F., Spahr, C. S., and Spector, D. L. (1999). Purification and biochemical characterization of interchromatin granule clusters. EMBO J. *18*, 4308–4320.

Mintz, P. J., and Spector, D. L. (2000). Compartmentalization of RNA processing factors within nuclear speckles. J. Struct. Biol. *129*, 241–251.

Misteli, T., and Spector, D. L. (1999). RNA polymerase II targets pre-mRNA splicing factors to transcription sites in vivo. Mol. Cell *3*, 697–705.

Moen, P. T., Jr., Johnson, C. V., Byron, M., Shopland, L. S., de la Serna, I. L., Imbalzano, A. N., and Lawrence, J. B. (2004). Repositioning of muscle-specific genes relative to the periphery of SC-35 domains during skeletal myogenesis. Mol. Biol. Cell *15*, 197–206.

Molenaar, C., Abdulle, A., Gena, A., Tanke, H. J., and Dirks, R. W. (2004). Poly(A)+ RNAs roam the cell nucleus and pass through speckle domains in transcriptionally active and inactive cells. J. Cell Biol. *165*, 191–202.

Mortillaro, M. J., Blencowe, B. J., Wei, X., Nakayasu, H., Du, L., Warren, S. L., Sharp, P. A., and Berezney, R. (1996). A hyperphosphorylated form of the large subunit of RNA polymerase II is associated with splicing complexes and the nuclear matrix. Proc. Natl. Acad. Sci. USA *93*, 8253–8257.

Myojin, R., Kuwahara, S., Yasaki, T., Matsunaga, T., Sakurai, T., Kimura, M., Uesugi, S., and Kurihara, Y. (2004). Expression and functional significance of mouse paraspeckle protein 1 on spermatogenesis. Biol. Reprod. *71*, 926–932.

Neugebauer, K. M., and Roth, M. B. (1997). Distribution of pre-mRNA splicing factors at sites of RNA polymerase II transcription. Genes Dev. *11*, 1148–1159.

Nguyen, V. T., Giannoni, F., Dubois, M. F., Seo, S. J., Vigneron, M., Kedinger, C., and Bensaude, O. (1996). In vivo degradation of RNA polymerase II largest subunit triggered by alpha-amanitin. Nucleic Acids Res. *24*, 2924–2929.

Ospina, J. K., and Matera, A. G. (2002). Proteomics: the nucleolus weighs in. Curr. Biol. *12*, R29–R31.

Patturajan, M., Schulte, R. J., Sefton, B. M., Berezney, R., Vincent, M., Bensaude, O., Warren, S. L., and Corden, J. L. (1998). Growth-related changes in phosphorylation of yeast RNA polymerase II. J. Biol. Chem. *273*, 4689–4694.

Phair, R. D., and Misteli, T. (2000). High mobility of proteins in the mammalian cell nucleus. Nature *404*, 604–609.

Pombo, A., Hollinshead, M., and Cook, P. R. (1999a). Bridging the resolution gap: imaging the same transcription factories in cryosections by light and electron microscopy. J. Histochem. Cytochem. *47*, 471–480.

Pombo, A., Jackson, D. A., Hollinshead, M., Wang, Z., Roeder, R. G., and Cook, P. R. (1999b). Regional specialization in human nuclei: visualization of discrete sites of transcription by RNA polymerase III. EMBO J. *18*, 2241–2253.

Puvion, E., and Puvion-Dutilleul, F. (1996). Ultrastructure of the nucleus in relation to transcription and splicing: roles of perichromatin fibrils and interchromatin granules. Exp. Cell Res. *229*, 217–225.

Schroeder, S. C., Schwer, B., Shuman, S., and Bentley, D. (2000). Dynamic association of capping enzymes with transcribing RNA polymerase II. Genes Dev. *14*, 2435–2440.

Schul, W., van Driel, R., and de Jong, L. (1998). Coiled bodies and U2 snRNA genes adjacent to coiled bodies are enriched in factors required for snRNA transcription. Mol. Biol. Cell *9*, 1025–1036.

Shopland, L. S., Johnson, C. V., Byron, M., McNeil, J., and Lawrence, J. B. (2003). Clustering of multiple specific genes and gene-rich R-bands around SC-35 domains: evidence for local euchromatic neighborhoods. J. Cell Biol. *162*, 981–990.

Shopland, L. S., Johnson, C. V., and Lawrence, J. B. (2002). Evidence that all SC-35 domains contain mRNAs and that transcripts can be structurally constrained within these domains. J. Struct. Biol. *140*, 131–139.

Spector, D. L., O'Keefe, R. T., and Jimenez-Garcia, L. F. (1993). Dynamics of transcription and pre-mRNA splicing within the mammalian cell nucleus. Cold Spring Harb. Symp. Quant. Biol. *58*, 799–805.

Sugaya, K., Vigneron, M., and Cook, P. R. (2000). Mammalian cell lines expressing functional RNA polymerase II tagged with the green fluorescent protein. J. Cell Sci. *113*, 2679–2683.

Warren, S. L., Landolfi, A. S., Curtis, C., and Morrow, J. S. (1992). Cytostellin: a novel, highly conserved protein that undergoes continuous redistribution during the cell cycle. J. Cell Sci. *103*, 381–388.

Wei, X., Somanathan, S., Samarabandu, J., and Berezney, R. (1999). Three-dimensional visualization of transcription sites and their association with splicing factor-rich nuclear speckles. J. Cell Biol. *146*, 543–558.

Xie, S. Q., and Pombo, A. (2005). Distribution of different phosphorylated forms of RNA polymerase II in relation to Cajal and PML bodies in human cells: an ultrastructural study. Histochem. Cell. Biol. *125*, 21–31.

Zeng, C., and Berget, S. M. (2000). Participation of the C-terminal domain of RNA polymerase II in exon definition during pre-mRNA splicing. Mol. Cell. Biol. *20*, 8290–8301.

Zeng, C., Kim, E., Warren, S. L., and Berget, S. M. (1997). Dynamic relocation of transcription and splicing factors dependent upon transcriptional activity. EMBO J. *16*, 1401–1412.

Zorio, D. A., and Bentley, D. L. (2004). The link between mRNA processing and transcription: communication works both ways. Exp. Cell Res. *296*, 91–97.

Supplemental Materials

"Splicing speckles are not reservoirs of RNA polymerase II, but contain an inactive form, phosphorylated on Serine2 residues of the CTD."

Sheila Q. Xie, Sonya Martin, Pascale V. Guillot, David L. Bentley and Ana Pombo

Labeling properties of antibodies to different forms of pol II.

Antibodies that detect total pol II outside the CTD (H224 and ARNA-3)

Antibodies H224 and ARNA3 bind to non-CTD domains of RPB1 (Figure 1A) and detect total pol II. As expected H224 and ARNA3 label both pol II_A and II_O bands in western blots of whole HeLa cell extracts with little other activities (Figure 1B).

Total pol II is found in discrete sites outside nucleoli, with a small number of brighter sites observed in some nuclear sections (Figure 1C,D). EGFP-pol II shows similar distribution (Sugaya *et al.*, 2000). H224 and ARNA3 also label the cytoplasm, where RPB1 is likely to be translated (Figure 1C,D; arrowheads). H224 also labels a small number of sites within nucleoli (Figure 1C, arrow); these may correspond to a minor cross-reactivity or non-specific background staining, as they are not detected with the CTD-specific antibodies (Figure 1F).

Antibodies that detect hypophosphorylated pol II (8WG16)

Antibody 8WG16 binds to unphosphorylated heptad repeats, and more weakly to Ser^5-phosphorylated repeats (Figure 1A; Patturajan *et al.*, 1998; Cho *et al.*, 2001; Doyle *et al.*, 2002). Phosphorylation on Ser^2 residues prevents binding of 8WG16 to CTD heptad repeats, whereas Ser^5 phosphorylation only partially reduces binding. 8WG16 has previously been used as a marker of total pol II (Bregman *et al.*, 1995), under the assumption that some unphosphorylated heptad repeats are present in most II_O molecules. However, in total protein extracts prepared in the presence of phosphatase inhibitors, 8WG16 detects little of the II_O band (Figure 1B; see also Doyle *et al.*, 2002). This indicates that the vast majority of pol II_O molecules in HeLa cells have most of its heptad repeats phosphorylated on Ser^2 and/or Ser^5. Pre-treatment of blots with AP confirms that phosphorylation, and not conformational changes on the CTD, prevent 8WG16 binding (not shown; see also Doyle *et al.*, 2002). As most pol II molecules detected by 8WG16 correspond

to the II_A form, 8WG16 is not a good marker of total pol II unless samples are pretreated with alkaline phosphatase.

Pol II_A is found in discrete sites throughout the nucleoplasm, with 1-3 brighter sites (see also Bregman *et al.*, 1995), and also a minor fraction in the cytoplasm (Figure 1E) as observed with antibodies H224 and ARNA3. As expected, pre-treatment of cryosections with alkaline phosphatase, in conditions that remove all detectable Ser^2P and Ser^5P epitopes (Figure 1H,J,L), increases the intensity of the nucleoplasmic signal detected by 8WG16 (by 1.5 fold; Figure 1F). The use of 8WG16 after alkaline phosphatase treatment is likely to significantly enhance the sensitivity of the immunofluorescence assay, as the epitope detected is present 42 times in the canonical CTD repeats. This experiment confirms that total pol II is found concentrated in discrete sites throughout the nucleoplasm.

Antibodies that detect pol II phosphorylated on Ser^5 residues of the CTD (rabbit anti-Ser^5P and 4H8)

Pol II phosphorylated on Ser^5 has previously been detected with antibody H14 (Patturajan *et al.*, 1998) and was found in discrete sites throughout the nucleoplasm (Bregman *et al.*, 1995; A.P., not shown). However, recent batches of this antibody give variable results (see also Komarnitsky *et al.*, 2000; Ahn *et al.*, 2004)); we found that the commercial form of this antibody does not give specific or sensitive staining of Ser^5P pol II in cryosections unlike the original formulation (not shown; Warren *et al.*, 1992). Different commercial batches were tested.

Alternative antibodies, rabbit anti-Ser^5P and 4H8, have recently become available. Rabbit anti-Ser^5P binds to CTD heptad-repeat tetramers containing Ser^5P, but not Ser^2P (Schroeder *et al.*, 2000). 4H8 is a commercial antibody raised against Ser^5P peptides, but is not fully characterized. 4H8 immunoprecipitates pol II at promoter sequences (Metivier *et al.*, 2004) and it detects pol II in discrete sites in mammalian cells (Osborne *et al.*, 2004). Although it has been reported that 4H8 detects both hypo- and hyperphosphorylated forms of pol II in yeast extracts (Kristjuhan *et al.*, 2002), our western analyses of human cell extracts prepared in the presence of phosphatase inhibitors show otherwise. In western blots, rabbit anti-Ser^5P and 4H8 detect the II_O band and a smear of faster migrating forms, but not the II_A band (Figure 1B; for equivalent results with antibody H14, see Zeng and

Berget, 2000). This suggests that most II_A molecules in HeLa cells are not phosphorylated on Ser^5 residues. Ser^5P pol II detected with either antibody is distributed in discrete nucleoplasmic sites and a few brighter sites (Figure 1G,I). Alkaline phosphatase treatment (Figure 1H,J) demonstrates the specificity of these two antibodies to phosphorylated epitopes.

Antibodies that detect pol II phosphorylated on Ser^2 residues of the CTD (H5)

Phosphorylation on Ser^2 correlates with transcription elongation and therefore is likely to be the best marker for active polymerase. Pol II phosphorylated on Ser^2 can be detected with antibody H5, with increased affinity when Ser^5 is also phosphorylated (Patturajan *et al.*, 1998; Cho *et al.*, 2001; Licatalosi *et al.*, 2002; Jones *et al.*, 2004). H5 exclusively detects the II_O band in whole cell extracts, but not the II_A form, or the intermediate smear that is detected by antibodies to Ser^5P (Figure 1B; see also Zeng and Berget, 2000).

Immunofluorescence analysis using H5 shows Ser^2P pol II_O in discrete sites throughout the nucleoplasm, with occasional brighter sites in some sections (Figure 1K; see also Warren *et al.*, 1992; Grande *et al.*, 1996; Pombo *et al.*, 1998; Guillot *et al.*, 2004); as expected, cytoplasmic (inactive) pol II is not phosphorylated on this epitope. Ser^2P pol II marked by H5 has previously been observed predominantly in splicing speckles (Bregman *et al.*, 1994; Bregman *et al.*, 1995; Zeng *et al.*, 1997; Mintz and Spector, 2000), but this distribution results from low-stringency fixation procedures or harsher permeabilization treatments that disrupt nuclear ultrastructure and induce loss of nuclear proteins (Guillot *et al.*, 2004). Alkaline phosphatase pre-treatment reveals the high specificity of H5 to phosphorylated epitopes (Figure 1L).

References

Ahn, S.H., Kim, M., and Buratowski, S. (2004). Phosphorylation of serine 2 within the RNA polymerase II C-terminal domain couples transcription and 3' end processing. Mol. Cell *13*, 67-76.

Bregman, D.B., Du, L., Li, Y., Ribisi, S., and Warren, S.L. (1994). Cytostellin distributes to nuclear regions enriched with splicing factors. J. Cell Sci. *107*, 387-396.

Bregman, D.B., Du, L., Van Der Zee, S., and Warren, S.L. (1995). Transcription-dependent redistribution of the large subunit of RNA polymerase II to discrete nuclear domains. J. Cell Biol. *129*, 287-298.

Cho, E.J., Kobor, M.S., Kim, M., Greenblatt, J., and Buratowski, S. (2001). Opposing effects of Ctk1 kinase and Fcp1 phosphatase at Ser 2 of the RNA polymerase II C-terminal domain. Genes Dev. *15*, 3319-3329.

Doyle, O., Corden, J.L., Murphy, C., and Gall, J.G. (2002). The distribution of RNA polymerase II largest subunit (RPB1) in the Xenopus germinal vesicle. J. Struct. Biol. *140*, 154-166.

Grande, M.A., van der Kraan, I., van Steensel, B., Schul, W., de The, H., van der Voort, H.T., de Jong, L., and van Driel, R. (1996). PML-containing nuclear bodies: their spatial distribution in relation to other nuclear components. J. Cell. Biochem. *63*, 280-291.

Guillot, P.V., Xie, S.Q., Hollinshead, M., and Pombo, A. (2004). Fixation-induced redistribution of hyperphosphorylated RNA polymerase II in the nucleus of human cells. Exp. Cell Res. *295*, 460-468.

Jones, J.C., Phatnani, H.P., Haystead, T.A., MacDonald, J.A., Alam, S.M., and Greenleaf, A.L. (2004). C-terminal repeat domain kinase I phosphorylates Ser2 and Ser5 of RNA polymerase II C-terminal domain repeats. J. Biol. Chem. *279*, 24957-24964.

Komarnitsky, P., Cho, E.J., and Buratowski, S. (2000). Different phosphorylated forms of RNA polymerase II and associated mRNA processing factors during transcription. Genes Dev. *14*, 2452-2460.

Kristjuhan, A., Walker, J., Suka, N., Grunstein, M., Roberts, D., Cairns, B.R., and Svejstrup, J.Q. (2002). Transcriptional inhibition of genes with severe histone H3 hypoacetylation in the coding region. Mol. Cell *10*, 925-933.

Licatalosi, D.D., Geiger, G., Minet, M., Schroeder, S., Cilli, K., McNeil, J.B., and Bentley, D.L. (2002). Functional interaction of yeast pre-mRNA 3' end processing factors with RNA polymerase II. Mol. Cell *9*, 1101-1111.

Metivier, R., Penot, G., Carmouche, R.P., Hubner, M.R., Reid, G., Denger, S., Manu, D., Brand, H., Kos, M., Benes, V., and Gannon, F. (2004). Transcriptional complexes engaged by apo-estrogen receptor-alpha isoforms have divergent outcomes. EMBO J. *23*, 3653-3666.

Mintz, P.J., and Spector, D.L. (2000). Compartmentalization of RNA processing factors within nuclear speckles. J. Struct. Biol. *129*, 241-251.

Osborne, C.S., Chakalova, L., Brown, K.E., Carter, D., Horton, A., Debrand, E., Goyenechea, B., Mitchell, J.A., Lopes, S., Reik, W., and Fraser, P. (2004). Active genes dynamically colocalize to shared sites of ongoing transcription. Nat. Genet. *36*, 1065-1071.

Patturajan, M., Schulte, R.J., Sefton, B.M., Berezney, R., Vincent, M., Bensaude, O., Warren, S.L., and Corden, J.L. (1998). Growth-related changes in phosphorylation of yeast RNA polymerase II. J. Biol. Chem. *273*, 4689-4694.

Pombo, A., Cuello, P., Schul, W., Yoon, J.B., Roeder, R.G., Cook, P.R., and Murphy, S. (1998). Regional and temporal specialization in the nucleus: a transcriptionally-active nuclear domain rich in PTF, Oct1 and PIKA antigens associates with specific chromosomes early in the cell cycle. EMBO J. *17*, 1768-1778.

Schroeder, S.C., Schwer, B., Shuman, S., and Bentley, D. (2000). Dynamic association of capping enzymes with transcribing RNA polymerase II. Genes Dev. *14*, 2435-2440.

Sugaya, K., Vigneron, M., and Cook, P.R. (2000). Mammalian cell lines expressing functional RNA polymerase II tagged with the green fluorescent protein. J. Cell Sci. *113*, 2679-2683.

Warren, S.L., Landolfi, A.S., Curtis, C., and Morrow, J.S. (1992). Cytostellin: a novel, highly conserved protein that undergoes continuous redistribution during the cell cycle. J. Cell Sci. *103*, 381-388.

Zeng, C., and Berget, S.M. (2000). Participation of the C-terminal domain of RNA polymerase II in exon definition during pre-mRNA splicing. Mol. Cell. Biol. *20*, 8290-8301.

Zeng, C., Kim, E., Warren, S.L., and Berget, S.M. (1997). Dynamic relocation of transcription and splicing factors dependent upon transcriptional activity. EMBO J. *16*, 1401-1412.

Supplemental Figure S1. Colocalization of Sm antigen, SC35 and polyA$^+$ RNA in the nucleus of HeLa cells. Cryosections were indirectly immunolabeled with antibodies against Sm antigen and/or SC35, prior to fluorescence *in situ* hybridization to polyA$^+$ RNA using a poly-dT probe. Higher magnification images of regions inside white boxes are shown on the right hand side of each lower magnification image. Bar, 2 μm.
(A) Sm antigen (red) and SC35 (green), (B) Sm antigen (red) and polyA$^+$ RNA (green), (C) SC35 (red) and polyA$^+$ RNA (green). As expected, the largest and brightest speckles labeled by the different markers coincide, although the labeling pattern is not strictly colocalized. Sm antigen (A,B) marks speckles and an interconnected meshwork, whilst SC35 (A,C) labels discrete domains with little interconnection. PolyA$^+$ RNA is found in discrete foci that are scattered throughout the nucleoplasm and cytoplasm, as expected for the distribution of polyadenylated mRNAs, and are enriched in “splicing speckles” (B,C).

Supplemental Figure S2. Using cryosections for quantitative immunofluorescence.
(A) Procedure. Tissues are fixed, embedded in a sucrose solution that acts as a cryoprotectant, and quickly frozen in liquid nitrogen. Ultrathin cryosections (100-150 nm thick) are cut on an ultracryomicrotome at –100ºC, thawed on a drop of sucrose and transferred to coverslips (for fluorescence microscopy). The sucrose that embeds the section is washed away before immunolabelling, and images are collected on a confocal microscope. The different cellular profiles present in a cryosection (along red lines; S1-4) originate from different cells in the tissue and represent the different parts of the nucleus. *Pale yellow*, cytoplasm; *blue*, nucleus; *aqua*, nucleoli; *green*, splicing speckles.
(B) Ultrastructure. The stringent fixation used to prepare cryosections (4 and 8% freshly-depolymerized paraformaldehyde in HEPES buffer; Guillot *et al.*, 2004) preserves the organization of cellular organelles at the ultrastructural level. Bar 500 nm.
(C) Immunofluorescence. Cryosections from cells grown in the absence (-) or presence (+) of α-amantin (α-am) were indirectly immunolabelled with antibodies against SC35 and Ser^{2}P pol II, and counterstained with TOTO-3 (pseudocoloured green, red and blue, respectively). Bar 5 μm.

(D) Quantification. The stereological quantification procedure summarized here provides information on the speckle content relative to the whole nucleoplasm (for pol II, splicing factors or polyA$^+$), and on the effects of the drug α-amanitin on nucleoplasm levels, partition in speckles and speckle volume. Note that this quantification is independent of the absolute thickness value, as section thickness (~100-150 nm) is much smaller than the size of speckles (~1 μm) and is equal throughout the nucleus. *px*, pixel; *au*, arbitrary units.

S.Q.Xie, Figure S1, Supplemental Data

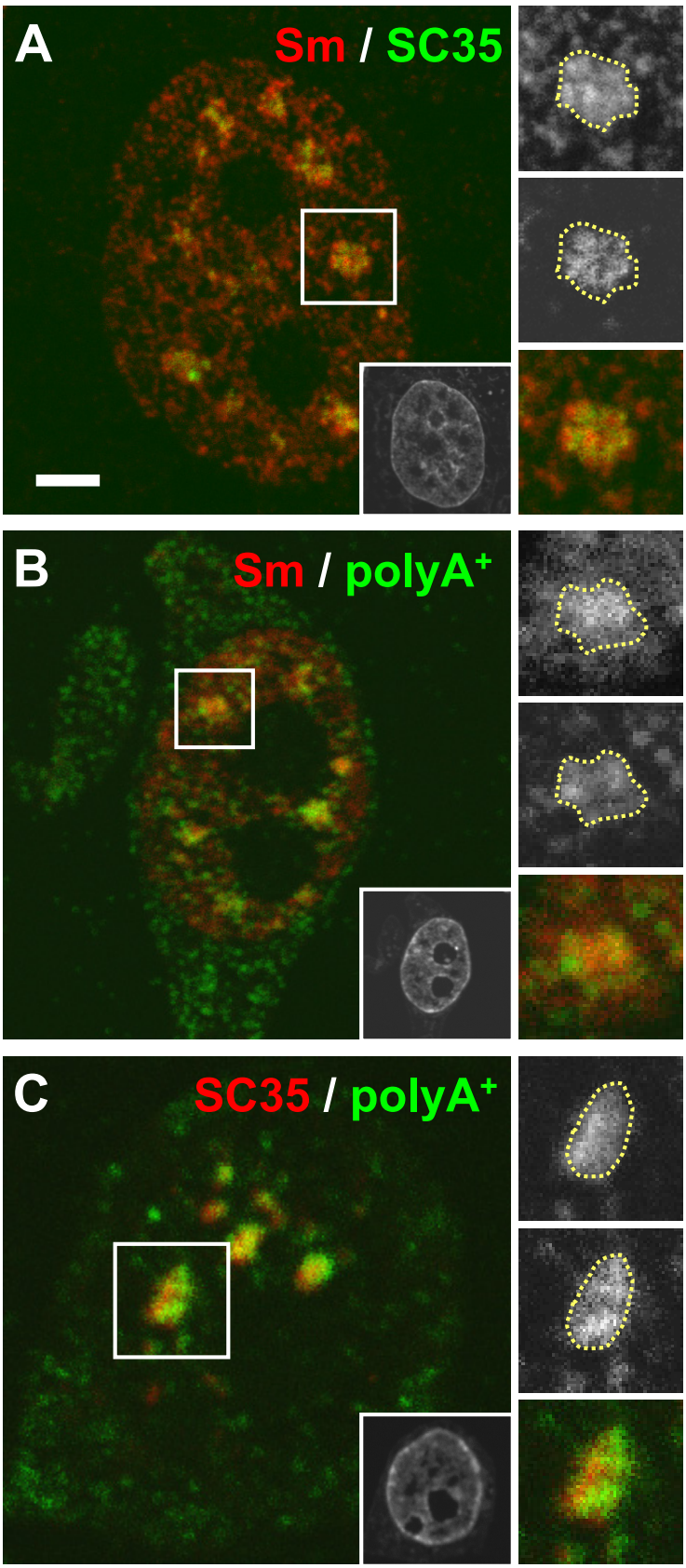

S.Q.Xie, Figure S2, Supplemental Data

A. Procedure

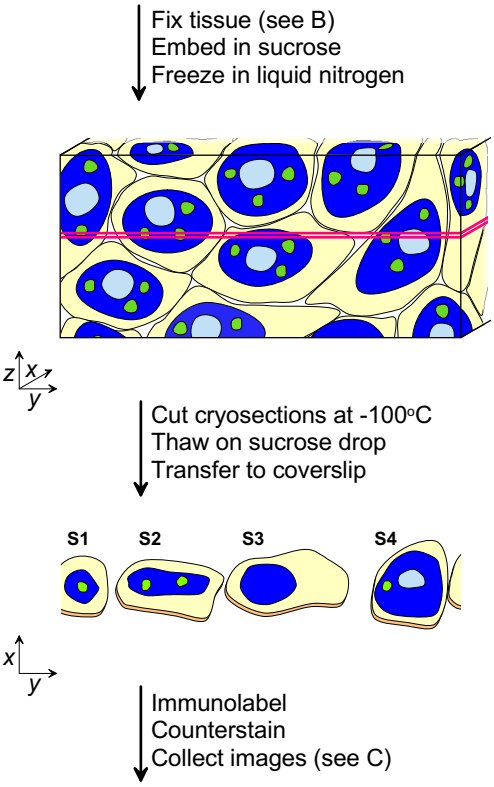

B. Ultrastructure

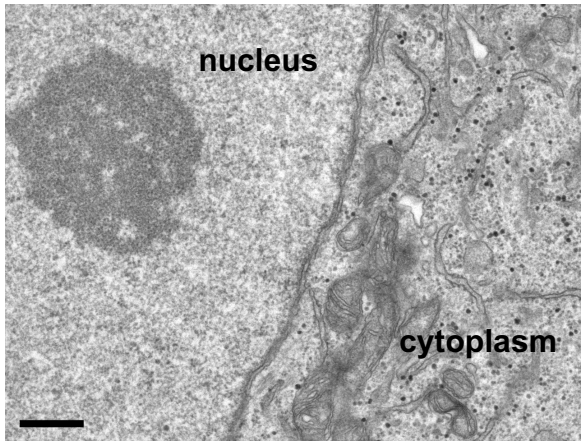

C. Immunofluorescence

DNA SC35 Ser²P

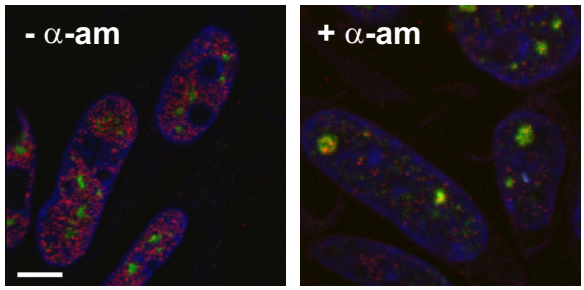

D. Quantification

1. Measure areas (A) and intensities (I) in nucleoplasm (np) and speckles for - and + α-am treated samples
2. Calculate average speckle volume, marker content in speckles (for pol II, splicing factors or polyA⁺), and average intensity in nucleoplasm

	Nucleoplasm			Speckles			Speckle Volume	Marker Content
	Area (*px*)	I (*au/px*)	T ($T_i=A_i \cdot I_i$)	Area (*px*)	I (*au/px*)	T ($T_i=A_i \cdot I_i$)	($Vs_i=\frac{As_i}{A_i} \cdot 100$; *%np*)	($Cs_i=\frac{Ts_i}{T_i} \cdot 100$; *%np*)
S1	A_1	I_1	T_1	As_1	Is_1	Ts_1	Vs_1	Cs_1
S2								
S3	...	...	...	...	...	...	...	...
...								
Sn	A_n	I_n	T_n	As_n	Is_n	Ts_n	Vs_n	Cs_n
Average		$\overline{I}=\frac{\sum I_i}{n}$					$\overline{Vs}=\frac{\sum Vs_i}{n}$	$\overline{Cs}=\frac{\sum Cs_i}{n}$

3. Normalize nucleoplasmic average intensity relative to untreated controls

$NI_{-\alpha\text{-am}} = 100$ $\qquad NI_{+\alpha\text{-am}} = \frac{\overline{I}_{+\alpha\text{-am}}}{\overline{I}_{-\alpha\text{-am}}} \cdot 100$

4. Normalize marker content relative to untreated controls

$NCs_{-\alpha\text{-am}} = \overline{Cs}_{-\alpha\text{-am}} \cdot NI_{-\alpha\text{-am}} / 100 = \overline{Cs}_{-\alpha\text{-am}}$ $\qquad NCs_{+\alpha\text{-am}} = \overline{Cs}_{+\alpha\text{-am}} \cdot NI_{+\alpha\text{-am}} / 100$

5. Graphical representation